

Magnetic, thermal and transport properties of a CePd₂Ga single crystal

This article has been downloaded from IOPscience. Please scroll down to see the full text article.

1995 J. Phys.: Condens. Matter 7 6899

(<http://iopscience.iop.org/0953-8984/7/34/013>)

View [the table of contents for this issue](#), or go to the [journal homepage](#) for more

Download details:

IP Address: 171.66.16.151

The article was downloaded on 12/05/2010 at 22:00

Please note that [terms and conditions apply](#).

Magnetic, thermal and transport properties of a CePd₂Ga single crystal

K Terayama, Y Aoki and H Sato

Department of Physics, Faculty of Science, Tokyo Metropolitan University, Hachioji-shi 192-03, Japan

Received 11 April 1995

Abstract. We have measured the electrical resistivity, thermoelectric power, magnetoresistance, magnetic susceptibility and magnetization of the antiferromagnetic Kondo lattice compound CePd₂Ga single crystal. A clear anisotropy and an antiferromagnetic transition at 2.9 K have been observed for both the electrical resistivity and the magnetic properties. The crystal-field level scheme has been investigated on the basis of the anisotropy and the magnetic specific-heat data; the first and the second excited states have been estimated to lie at 66 K and about 280 K, respectively.

1. Introduction

The intermetallic compound CePd₂Ga crystallizes in the orthorhombic YPd₂Si-type structure (space group, *Pnma*; *Z* = 4) [1]. The electrical resistivity, magnetic susceptibility and magnetization of CePd₂Ga were first studied by Das *et al* [2] on a polycrystalline sample. They reported an antiferromagnetic (AF) transition at 3.2 K, below which they observed a metamagnetic-like behaviour of the magnetization. From the electrical resistivity measurement, they judged this compound to be an AF Kondo lattice.

A large anisotropy in the physical properties is expected in this compound because of its orthorhombic structure. This means that experimental work on single-crystal samples is essential to determine the intrinsic properties of this materials. In this paper, we report the first measurements of the electrical resistivity ρ , thermoelectric power S , magnetoresistance, specific heat C , magnetic susceptibility χ and magnetization M on a single-crystal sample of CePd₂Ga. The results were analysed taking into account both the crystal-field effect and the Kondo effect.

2. Experimental details

Polycrystalline samples of CePd₂Ga and LaPd₂Ga were prepared by arc melting buttons with CePd₂Ga_{1.04} and LaPd₂Ga_{1.04}, taking into account a small Ga loss. The polycrystalline samples obtained are rather porous and brittle. A single crystal of CePd₂Ga was grown by the Czochralski pulling method in an argon atmosphere using a tri-arc furnace. The purities of the starting elements were as follows 99.9% Ce, 99.9% La, 99.99% Pd and 99.9999% Ga.

The electrical resistivity was measured by the ordinary DC four-probe method. The thermoelectric power was measured by the differential method applying the temperature

gradient along the a axis. The voltage measurements were made automatically with Keithley 181 nanovoltmeters using a microcomputer. The magnetic measurements were made with a Quantum Design SQUID magnetometer up to 5.5 T. The specific heat was measured by the adiabatic heat-pulse method.

3. Results and discussion

Figure 1 shows the temperature dependence of the inverse magnetic susceptibility χ^{-1} , which approximately follows the Curie–Weiss law above 20 K, 50 K and 100 K for the a axis (χ_a), b axis (χ_b) and c axis (χ_c), respectively. The effective Bohr magneton μ_{eff} and paramagnetic Curie temperature Θ_P are estimated to be $2.54\mu_B$ and 0 K for the a axis, $2.46\mu_B$ and -19 K for b axis and $2.57\mu_B$ and -44 K for the c axis. These μ_{eff} -values are close to $2.54\mu_B$ for the free Ce^{3+} ion. The low-temperature part of χ is shown in the inset. χ_a is larger than both χ_b and χ_c , and exhibits a clear peak at 2.9 K, suggesting an AF transition with the magnetic easy direction along the a axis. The transition temperature is somewhat lower than the Néel temperature of 3.2 K reported for a polycrystalline sample [2]. A small peak has been observed also for χ_b and χ_c near $T_N = 2.9$ K.

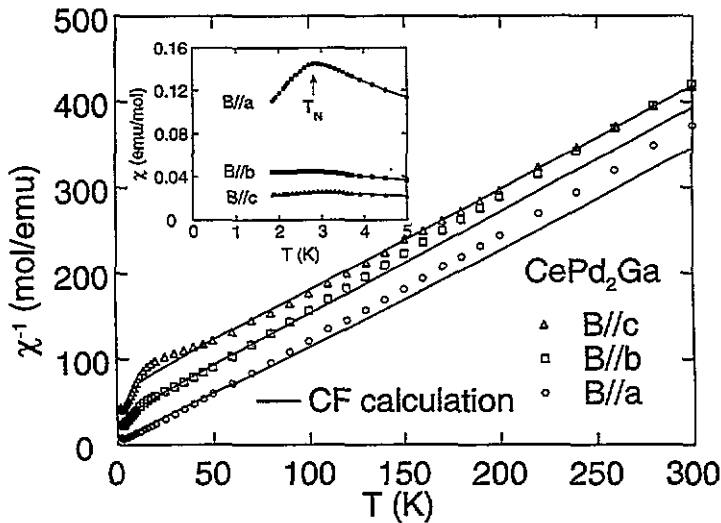


Figure 1. Temperature dependence of the inverse magnetic susceptibility χ : — CF calculation. The inset is the low-temperature part of $\chi(T)$.

Figure 2 shows the field dependence of magnetization at 2 K ($< T_N$) and 5 K ($> T_N$). At 2 K, the magnetization (M_a) along the a axis shows a metamagnetic-like behaviour near 2.5 T and reaches $1.3\mu_B/Ce$ at 5.5 T, which is consistent with the AF coupling with the magnetic easy axis along the a axis. The magnetization curve for $B \parallel a$ is close to that reported for the polycrystalline sample [2], which can be explained if their sample accidentally had a large grain with $a \parallel B$. For $B \parallel c$, we see a slight upturn in M above 4 T possibly due to a metamagnetic transition. The observed anisotropy in M and χ is thought to be due to the crystal-field (CF) effect.

Figure 3 shows the specific heat C of $CePd_2Ga$ and $LaPd_2Ga$. For $LaPd_2Ga$, the Sommerfeld coefficient and Debye temperature, estimated from the C/T versus T^2 plot (not shown), are $\gamma = 6$ mJ K $^{-2}$ mol $^{-1}$ and $\Theta_D = 244$ K, respectively. The specific heat for

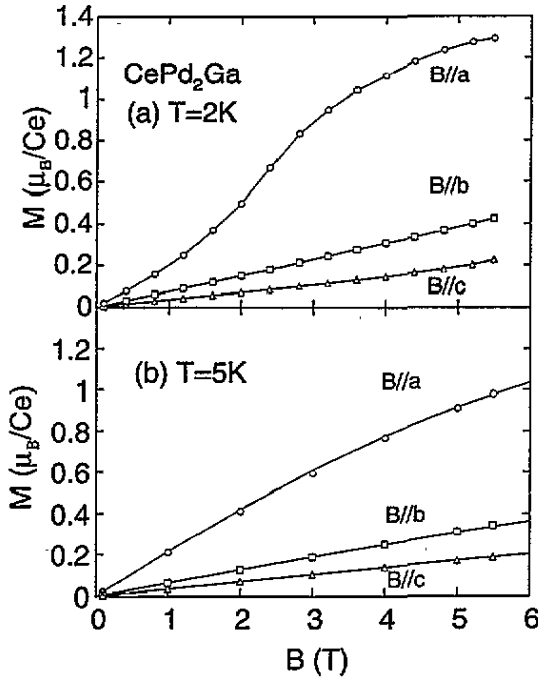


Figure 2. Magnetization curves at (a) 2 K and (b) 5 K.

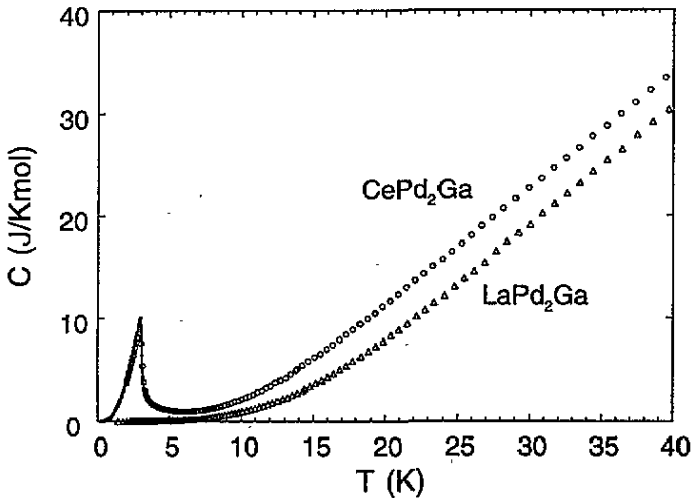


Figure 3. Temperature dependences of the specific heat C for $CePd_2Ga$ and $LaPd_2Ga$.

$CePd_2Ga$ is larger than that for $LaPd_2Ga$ due to the magnetic contribution of 4f electrons. A λ -type anomaly corresponding to the AF transition is observed at low temperatures. Figure 4 shows the comparison of the specific-heat data between the single-crystal and polycrystalline samples of $CePd_2Ga$ at low temperatures. The data for the single-crystal sample show a clearer transition than the data for the polycrystalline sample do. In order to estimate the γ -value in the AF state, C/T was plotted against T^2 at low temperatures in the inset. From the linear variation below 500 mK, the electronic specific coefficient was estimated to be

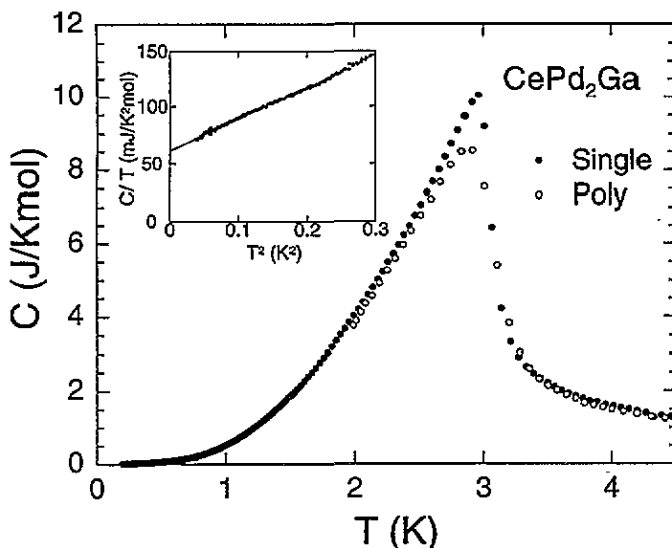


Figure 4. Specific heats of the polycrystalline and single-crystal samples of CePd_2Ga around T_N . The inset shows a plot of C/T against T^2 at low temperatures.

$\gamma = 63 \text{ mJ K}^{-2} \text{ mol}^{-1}$. The observed T^3 term in this temperature region is due to the AF magnon excitation and has a coefficient of $270 \text{ mJ K}^{-4} \text{ mol}^{-1}$; the T^3 coefficient for the phonon part estimated from the data on LaPd_2Ga is negligibly small ($0.54 \text{ mJ K}^{-4} \text{ mol}^{-1}$).

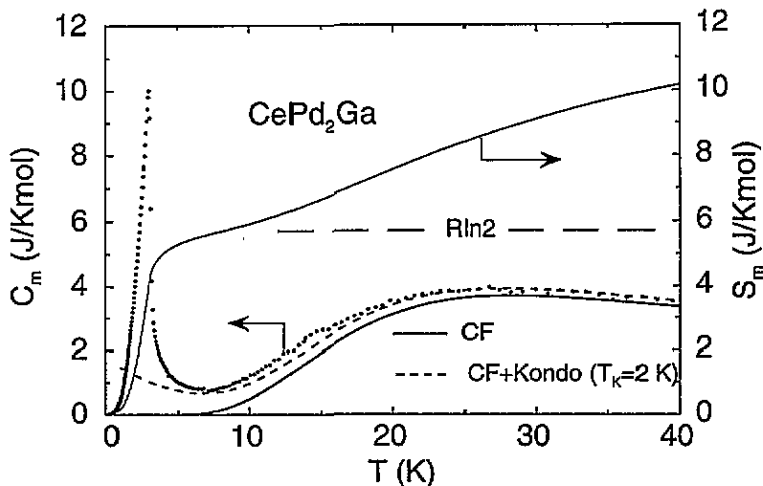


Figure 5. Magnetic contribution of the specific heat C_m : — theoretical curve for the CF excitation model, --- theoretical curve for the $s = \frac{1}{2}$ Kondo model of $T_K = 2 \text{ K}$ and the CF excitation model. The magnetic entropy $S_m(T)$ is also shown.

The magnetic contribution to the specific heat $C_m = C(\text{CePd}_2\text{Ga}) - C(\text{LaPd}_2\text{Ga})$ is shown in figure 5. The broad peak at around 25 K may be due to the CF excitation. The magnetic entropy S_m , obtained by integrating C_m/T , is also shown in figure 5. With increasing temperature, S_m increases rapidly below T_N to approach $0.73R \ln 2$ at T_N and shows a plateau with the approximate value of $R \ln 2$ near $T = 10 \text{ K}$. At higher temperatures,

S_m starts to increase again probably due to the CF excitation corresponding to the broad peak at around 25 K in C_m . The Ce^{3+} ions occupy the equivalent monoclinic sites (C_{1h}) in the YPd_2Si -type crystal structure. Due to the CF effect, the sixfold-degenerate states of 4f electron in Ce^{3+} with the total angular momentum $J = \frac{5}{2}$ splits into three doublets. The increase in S_m for $S_m > R \ln 2$ is caused by the thermal CF excitation to the first excited-state doublet from the ground state doublet. From the maximum temperature of 25 K, we estimated the first excited state to lie at $\Delta_1 \simeq 60$ K. In the region of $S_m < R \ln 2$ the degeneracy in the ground-state doublet is lifted, mainly due to the AF transition as evidenced by $S_m(T_N) = 0.73R \ln 2$.

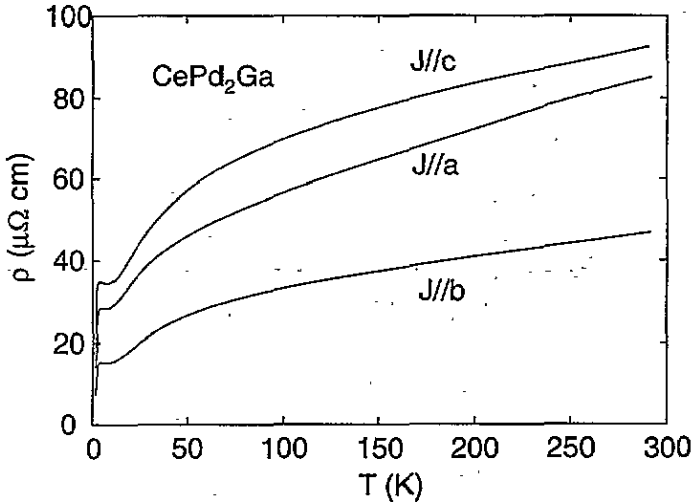


Figure 6. The temperature dependence of the electrical resistivity for the single-crystal sample of $CePd_2Ga$.

Figure 6 shows the temperature dependence of the electrical resistivity ρ on a $CePd_2Ga$ single crystal for currents i along the three principal axes. On the whole, the temperature dependences are similar although the absolute value largely depends on the directions. The electrical resistivity shows a subtle increment below 8 K with decreasing T , suggesting the Kondo scattering. The sudden drop in the electrical resistivity below 3 K is due to AF ordering.

The temperature dependence of the thermoelectric power $S(T)$ is shown in figure 7. The thermoelectric power decreases with decreasing temperature from about $13 \mu V K^{-1}$ at room temperature, changes its sign to negative near 30 K and shows a minimum at $T_{min} = 8$ K. Similar temperature dependences have been reported for typical AF Kondo lattice compounds such as $CeAl_2$ and $CeCu_2$ [3]. We can estimate $T_K \simeq 4$ K for $CePd_2Ga$ if we use the relation $T_{min} \simeq \frac{1}{2}T_K$ [4]. The shoulder at around 50 K is possibly due to both the Kondo effect and the CF effect [5].

Figure 8 shows the low-temperature part of the electrical resistivity at 0, 1 and 5 T. The magnetoresistance is always negative at 5 T. The inset shows the temperature dependence of the longitudinal magnetoresistance $\Delta\rho/\rho = \{\rho(B = 1 T) - \rho(B = 0 T)\}/\rho(B = 0 T)$. The negative peak at 3 K is correlated with the AF transition. The negative magnetoresistance observed above T_N has two possible origins: the suppression of Kondo effect and/or the spin fluctuation due to the field. Taking into account the negative temperature derivative of ρ above T_N , we infer that the former is dominant in the present case. The field

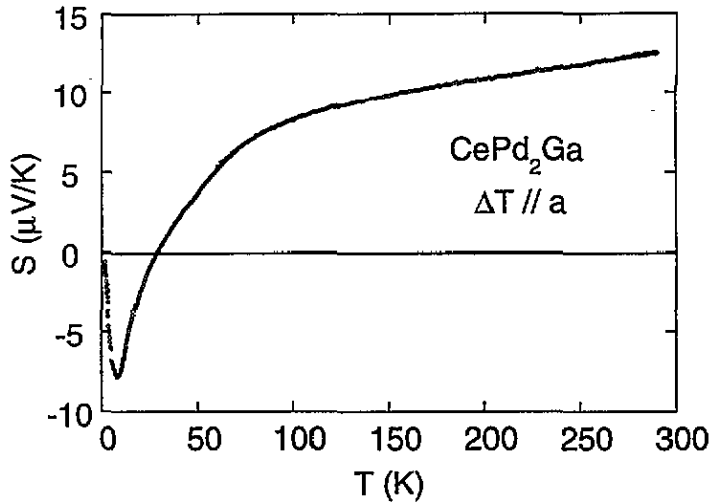


Figure 7. Temperature dependence of the thermoelectric power S .

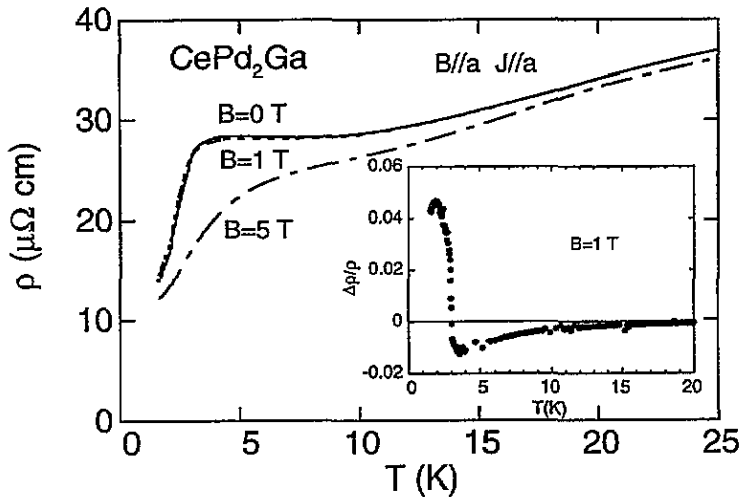


Figure 8. Temperature dependence of the electrical resistivity at 0, 1 and 5 T for field and current along the a axis. The derived magnetoresistance at 1 T is shown in the inset.

dependences of the longitudinal magnetoresistance at 2 K and 5 K are shown in figure 9. At 5 K, $\Delta\rho/\rho$ monotonically decreases. If the negative magnetoresistance is mainly due to the Kondo effect, $\Delta\rho/\rho$ is related to the magnetization as $\Delta\rho/\rho \propto -M^2$ in the single-ion Kondo model [6]. In order to test the relation, we compared $\Delta\rho/\rho$ with $-\alpha M^2$ using a constant α normalized at $B = 5$ T. The field dependence can be approximately reproduced, which partly supports the dominance of Kondo scattering above T_N . At 2 K, the magnetoresistance first increases with increasing field and starts to decrease after showing a peak near $B_M = 2.8$ T. The magnetoresistance changes its sign above 4 T. The peak is correlated with the metamagnetic transition in the $M(B)$ curve shown in figure 2(a). Such behaviour of the magnetoresistance is qualitatively consistent with the theoretical calculation given by Yamada and Takada [7]. In the AF state ($B < B_M$), the magnetic moment fluctuation in one magnetic sublattice is enhanced by the field while, in the field-

induced ferromagnetic state ($B > B_M$), the fluctuation is suppressed by the field. The change in the fluctuation is reflected in the magnetoresistance.

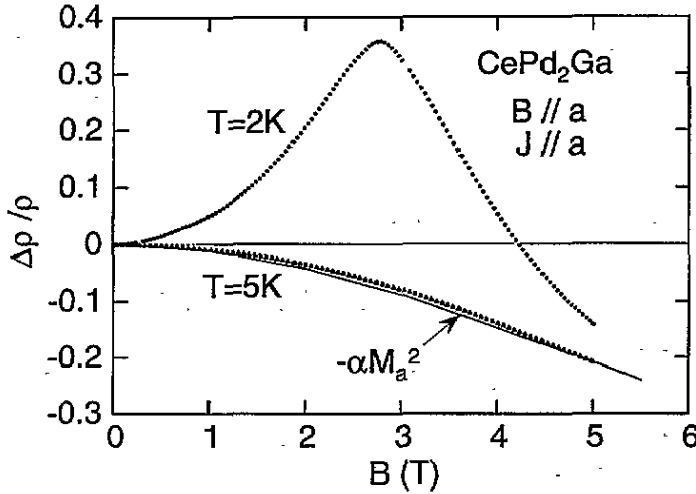


Figure 9. Magnetic field dependences of the longitudinal magnetoresistance along the a axis at 2 K and 5 K.

The crystal anisotropy of CePd₂Ga is reflected in the magnetic susceptibility χ , the magnetization M , and the electrical resistivity ρ mainly by way of the (CF) effect. We try to analyse the $\chi(T)$, $M(B)$ and $C(T)$ data in the paramagnetic state using the CF model. In the monoclinic site symmetry (C_{1h}), the single-ion CF Hamiltonian is given by

$$H_{CF} = B_2^0 O_2^0 + B_2^2 O_2^2 + B_4^0 O_4^0 + B_4^2 O_4^2 + B_4^{-2} O_4^{-2} + B_4^4 O_4^4 + B_4^{-4} O_4^{-4} \quad (1)$$

where B_j^i and O_j^i are the CF parameters and the Stevens operator equivalents, respectively. In order to consider the RKKY interaction between the Ce³⁺ magnetic moments in the molecular-field approximation, we use the following Hamiltonian:

$$H = H^{CF} - g\mu_B J_i (H_i + H_i^{MF}) + \frac{1}{2} \lambda_P M_i^2 \quad (2)$$

where H_i^{MF} and M_i are the molecular field and the thermally averaged magnetization of the Ce³⁺ ion, respectively, for the field along a local i axis. The molecular field is given by

$$H_i^{MF} = \lambda_P M_i = \lambda_P g\mu_B \langle J_i \rangle. \quad (3)$$

By the diagonalization of equation (2), we can obtain the set of eigenfunctions and eigenvalues as well as M_i , from which we calculate χ^{CF} and $C(T)$. The observed χ should be compared with the calculated value of

$$\frac{1}{\chi} = \frac{1}{\chi^{CF}} - \lambda_P \quad (4)$$

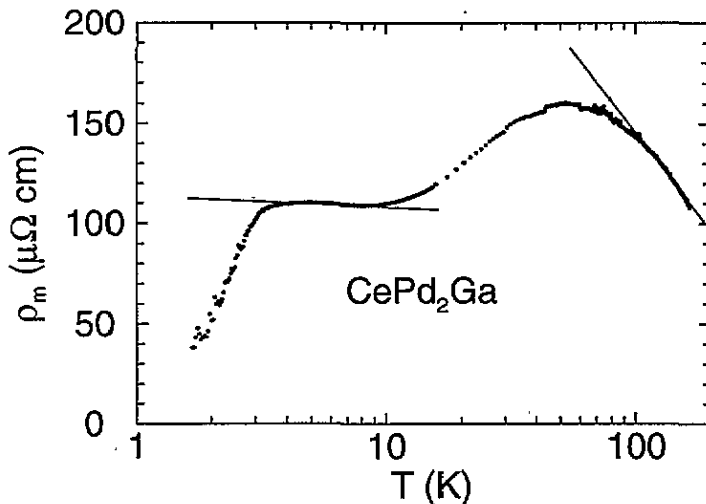
where λ_P is a molecular-field constant. We refined the CF parameters B_j^i and λ_P by the least-squares fitting method using $\chi(T)$ and $C(T)$ data. The best-fit results are as in table 1; however, neutron scattering experiments are necessary to confirm the reliability of the set of parameters.

The calculated results using the parameters are shown in figures 1 and 5 as the solid curves. The calculated χ^{-1} is well reproduced over all the anisotropy in the experiment,

Table 1. Results of the CF analysis for CePd₂Ga.

$B_2^0 = +1.29$ K	$B_2^2 = +9.67$ K	$B_4^0 = +0.13$ K	$B_4^2 = +0.93$ K
$B_4^{-2} = +3.51$ K	$B_4^4 = +1.36$ K	$B_4^{-4} = -0.78$ K	$\lambda_P = -0.84$ mol emu ⁻¹
Second excited state	$\Delta_2 \simeq 280$ K		
First excited state	$\Delta_1 = 66$ K		

although the deviation is large at higher temperatures for the *a* and *b* axes. The difference between the experimental and calculated values for the specific heat may be due to the Kondo effect, which was neglected in the present calculation. In the magnetic Kondo systems, assuming that the remaining entropy compared with $R \ln 2$ is caused by the Kondo effect, we usually estimate the Kondo temperature T_K from the entropy at the magnetic transition temperature: $S_m(T_N) = S_K(T_N/T_K)$, where $S_K(T_N/T_K)$ is the Kondo entropy at T_N [8]. From the experimental value of $S_m(T_N) = 0.73R \ln 2$, we obtained $T_K = 2$ K which is same order of magnitude as that determined from the thermoelectric power. To estimate the Kondo contribution to $C_m(T)$, we usually use the numerical results from the Bethe *ansatz* in the spin- $\frac{1}{2}$ Kondo model by Desgranges and Schotte [9]. If we add this theoretical Kondo contribution with $T_K = 2$ K to the CF contribution, the observed $C_m(T)$ above 6 K can be well reproduced as shown in figure 4 with a broken curve.

**Figure 10.** Magnetic contribution of resistivity estimated from the polycrystalline data.

To determine the CF effect on the electrical resistivity, we plot in figure 10 the magnetic contribution of the resistivity, $\rho_m = \rho(\text{CePd}_2\text{Ga}) - \rho(\text{LaPd}_2\text{Ga})$, using the polycrystalline data. Besides the Kondo behaviour in ρ_m in the region of $T_N < T < 10$ K, we can see a broad peak near 50 K. This anomaly is probably due to the Kondo scattering accompanying the CF effect. Hanzawa *et al* [10] proposed that T_K is modified by the CF effect at high temperatures as $T_K^h = (\Delta_1 \Delta_2 T_K)^{1/3}$. In several typical Kondo compounds, it was reported that the temperature at the resistivity peak roughly agrees with T_K^h . Using the CF level scheme determined above, we estimated T_K^h to be 42 K, which roughly agrees with the peak temperature of 50 K.

4. Summary

Using the experimental results on transport, magnetic and thermal properties in single-crystal samples, we analysed the 4f electron state in CePd₂Ga. The overall properties of CePd₂Ga are well explained by the combined model including the (CF) effect and Kondo effect. The estimated T_K , of the order of 2–4 K, is comparable with the AF transition temperature $T_N = 2.9$ K, suggesting the delicate competition between the Kondo effect and RKKY interaction.

Acknowledgment

This work was partly supported by a Grant-in-Aid for Scientific Research from The Ministry of Education, Science and Culture of Japan.

References

- [1] Hulliger F, Mattenberger K and Siegrist S 1992 *J. Alloys Compounds* **190** 125
- [2] Das I, Sampathkumaran E V, Chari S and Gopalakrishnan K V 1993 *J. Alloys Compounds* **202** L7
- [3] Satoh K, Fukuda A, Umehara I, Ōnuki Y, Sato H and Takayanagi S 1992 *J. Phys. Soc. Japan* **61** 3267
- [4] Gratz E, Bauer E, Barbara B, Zemirli S, Steglich F, Bredl C D and Lieke W 1985 *J. Phys. F: Met. Phys.* **15** 1975
- [5] Maekawa S, Kashiba S, Tachiki M and Takahashi S 1986 *J. Phys. Soc. Japan* **55** 3194
- [6] Yosida K and Yoshimori A 1973 *Magnetism* vol 5, ed H Suhl (New York: Academic) p 253
- [7] Yamada H and Takada S 1973 *Prog. Theor. Phys.* **49** 1401
- [8] Mori H, Yashima H and Sato N 1985 *J. Low Temp. Phys.* **58** 513
- [9] Desgranges H U and Schotte K D 1982 *Phys. Lett.* **91A** 240
- [10] Hanzawa K, Yamada K and Yoshida K 1985 *J. Magn. Magn. Matter.* **47–8** 357